Robust Quantity-Aware Aggregation for Federated Learning

Jingwei Yi[1], Fangzhao Wu[2], Huishuai Zhang[2], Bin Zhu[2], Guangzhong Sun[1], Xing Xie[2]
[1]University of Science and Technology of China, Hefei 230027, China
[2]Microsoft Research Asia, Beijing 100080, China
yjw1029@mail.ustc.edu.cn,gzsun@ustc.edu.cn,{fangzwu,huzhang,binzhu,xingx}@microsoft.com

arXiv:2205.10848v2 [cs.CR] 26 Jul 2023

ABSTRACT

Federated Learning (FL) enables multiple clients to collaborate on training machine learning models without sharing their data, making it an important privacy-preserving framework. However, FL is susceptible to security and robustness challenges, such as malicious clients potentially corrupting model updates and amplifying their impact through excessive quantities. Existing defenses for FL, while all handling malicious model updates, either treat all quantities as benign or ignore/truncate quantities from all clients. The former is vulnerable to quantity-enhanced attacks, while the latter results in sub-optimal performance due to the varying sizes of local data across clients. In this paper, we introduce a robust quantity-aware aggregation algorithm for FL called FedRA. FedRA considers local data quantities during aggregation and defends against quantity-enhanced attacks. It consists of two crucial components, i.e., a quantity-robust scorer and a malicious client number estimator. More specifically, the quantity-robust scorer calculates the sum of the distance between one update and the rest of the updates as the quantity-robust score, taking into account their quantities as factors. The malicious client number estimator uses these scores to predict the number of suspicious clients to exclude in each round, adapting to the dynamic number of malicious clients participating in FL in each round. Experiments on three public datasets demonstrate FedRA's effectiveness in defending against quantity-enhanced attacks in FL. The code for FedRA can be found at https://anonymous.4open.science/r/FedRA-4C1E.

CCS CONCEPTS

• **Security and privacy → Privacy protections**; • **Computing methodologies → Cooperation and coordination**; **Distributed artificial intelligence**.

KEYWORDS

robustness, federated learning, quantity

ACM Reference Format:
Jingwei Yi, Fangzhao Wu, Huishuai Zhang, Bin Zhu, Guangzhong Sun, Xing Xie. 2018. Robust Quantity-Aware Aggregation for Federated Learning. In *Proceedings of 29th ACM SIGKDD Conference on Knowledge Discovery and Data Mining (KDD '23).* ACM, New York, NY, USA, 14 pages. https://doi.org/XXXXXXX.XXXXXXX

Permission to make digital or hard copies of all or part of this work for personal or classroom use is granted without fee provided that copies are not made or distributed for profit or commercial advantage and that copies bear this notice and the full citation on the first page. Copyrights for components of this work owned by others than ACM must be honored. Abstracting with credit is permitted. To copy otherwise, or republish, to post on servers or to redistribute to lists, requires prior specific permission and/or a fee. Request permissions from permissions@acm.org.
KDD '23, August 6-10, 2023, Long Beach, CA, USA
© 2018 Association for Computing Machinery.
ACM ISBN 978-1-4503-XXXX-X/18/06…$15.00
https://doi.org/XXXXXXX.XXXXXXX

1 INTRODUCTION

Federated learning (FL) is an important technology to train models while protecting the privacy of training data. It has been extensively studied for various application scenarios, such as medical health [13, 22, 30, 32, 38] and keyboard next-word prediction [5, 9, 17, 27, 39]. One of the classic FL algorithms is FedAvg [21]. In FedAvg, the server iteratively averages clients' updates with some weights determined by the *quantity* of each client, which means throughout the paper the number of the training data at that client, to update the global model.

The linear aggregation used in FedAvg has been shown to be vulnerable to poisoning attacks [1–3, 8, 19, 34, 36]. These attacks primarily aim to either deteriorate the performance of the global model or insert a backdoor into the global model. However, malicious clients can also submit large quantities to obtain unfairly high weights in the model aggregation, leading to a heightened impact of their malicious updates on the global model. We refer to this type of attack as **quantity-enhanced attacks**.

Several methods have been proposed to defend against poisoning attacks for federated learning [4, 7, 25, 26, 33, 40]. These defenses can be categorized into three groups: quantity-ignorant, quantity-aware, and quantity-robust defenses. **Quantity-ignorant** defenses aggregate updates without considering quantities [4, 7, 40]. These methods are robust to quantity-enhanced attacks. However, since aggregating updates with quantities benefits model performance [28, 41], applying these defenses may lead to performance degradation. **Quantity-aware** defenses aggregate updates with quantities but by default treat quantities submitted by clients as benign [25, 33]. These defenses outperform quantity-ignorant defenses when there are no attacks, but their performance deteriorates significantly when faced with quantity-enhanced attacks. **Quantity-robust** defenses aggregate updates with quantities and, unlike quantity-aware defenses, are robust to quantity-enhanced attacks. Portnoy et al. [26] propose to truncate quantities with a dynamic threshold and apply quantity-aware Trimean [40] to aggregate updates. However, it handles updates and quantities separately, which could result in the truncation of the quantities of benign clients, ultimately leading to sub-optimal performance.

Meanwhile, some existing defenses [4, 7, 40] need a parameter that represents the upper bound of the number of malicious clients to be filtered out in each round. However, in cross-device federated learning, due to the large number of clients, only a subset of clients is selected for participation in each round. As a result, the number of malicious clients in each round changes dynamically. Over-estimating the number of malicious clients leads to some benign clients being filtered out, while underestimating the number of malicious clients may result in some malicious updates being included in the model aggregation.

In this paper, we propose *FedRA*, a quantity-robust defense for federated learning. It filters out malicious clients by taking both quantities and updates into consideration. More specifically, FedRA consists of two components, i.e., quantity-robust scorer and malicious client number estimator. The quantity-robust scorer is based on the observation that the expectation of distance between benign updates with larger quantities should be smaller. Therefore, to compute the quantity-robust score, we calculate the sum of distances between one update and the rest of the updates, taking into account the quantities as coefficients. The coefficient is smaller when the pair of quantities are larger. The malicious client number estimator uses the quantity-robust scores as input and predicts the number of malicious clients to exclude in each round by maximizing the log-likelihood. Finally, the corresponding number of updates with the largest quantity-robust scores are filtered out. The rest updates are aggregated with weights proportional to their quantities to update the global model.

The main contributions of this paper are as follows:

- We propose a robust quantity-aware aggregation method for federated learning to aggregate updates with quantities while defending against quantity-enhanced attacks.
- We theoretically prove FedRA is quantity-robust by proving its aggregation error is irrelevant to malicious quantities.
- We conduct experiments on three public datasets to validate the effectiveness of FedRA.

2 RELATED WORKS

2.1 Federated Learning

Federated learning [21] enables multiple clients collaboratively train models without sharing their local datasets. There are three steps in each round of federated learning. First, a central server randomly samples a group of clients and distributes the global model to them. Second, the selected clients train the model with their local datasets and upload their model updates to the central server. Finally, the central server aggregates the received updates to update the global model. In FedAvg [21], updates are weight-averaged according to the quantity of each client's training samples. Reddi et al. [28] have proposed FedAdam, where the server updates the global model with Adam optimizer. The above steps are performed iteratively until the global model converges.

2.2 Federated Poisoning Attacks

However, classical federated learning is vulnerable to poisoning attacks, e.g., untargeted attacks [2, 8] and backdoor attacks [1, 3, 19, 34, 37]. In this paper, we focus on defending against untargeted attacks, which aim to degrade the performance of the global model on arbitrary input samples. Label flip [8] is a data-poisoning-based untargeted attack, where the malicious clients manipulate the labels of their local training dataset to generate malicious updates. Some advanced attacks assume the malicious clients have knowledge of benign datasets and can collaborate to generate malicious updates. LIE [2] adds small noises to the average of benign updates to circumvent defenses. Optimize [8] models the attack as an optimization problem and adds noises in the opposite direction of benign updates. These attacks focus on generating malicious updates, but overlook the attacker can submit large quantities to obtain unfairly high weight in model aggregation.

2.3 Robust Aggregations

To defend against untargeted attacks in federated learning, several robust aggregation methods have been proposed. Yin et al. [40] propose Median and Trimean that apply coordinate-wise median and trimmed-mean, respectively, to filter out malicious updates. Blanchard et al. [4] propose Krum and mKrum that compute square-distance-based scores to select and average the updates closest to a subset of neighboring updates. Bulyan [7] is a combination of mKrum and Trimean: it first selects several updates through mKrum and then aggregates them with Trimean. We note that the above defense methods do not consider quantities of clients' training samples, which we categorize as *quantity-ignorant* methods, and the convergence speeds and model performance of these methods are compromised [28, 41], especially for quantity-imbalanced scenarios, such as long-tailed data distributions that are common in real-world scenarios [15, 42, 43].

Sun et al. [33] propose Norm-bound that clips the L^2 norm of received updates to a predefined threshold. Pillutla et al. [25] propose RFA that computes weights for each update by running an approximation algorithm to minimize the quantity-aware geometric median of updates. These two methods are categorized into *quantity-aware* defenses. They take quantities into consideration when aggregating updates but by default treat all received quantities as benign. Portnoy et al. [26] point out that received quantities may be malicious and can be exploited to increase the impact of malicious updates. They further propose a Truncate method that truncates received quantities within a dynamic threshold in each round, which guarantees any 10% clients do not have more than 50% samples. The Truncate method is categorized into *quantity-robust* method. However, quantities of benign clients with a large number of training samples may also be truncated, resulting in degraded performance. Meanwhile, they handle the malicious update filtering and the quantity truncation separately, which is sub-optimal.

3 PROBLEM DEFINITION

Suppose that training samples are sampled from a distribution $\mathcal{D}$ in sample space $\mathcal{Z}$. Let $f(\mathbf{w}; z)$ denote the loss function of model parameter $\mathbf{w} \in \mathcal{W}$ at data point z, and $F(\mathbf{w}) = \mathbb{E}_{z\sim\mathcal{D}}[f(\mathbf{w}; z)]$ is the corresponding population loss function. The goal is to minimize the population loss by training the model parameter, i.e., $\mathbf{w}^* = \arg\min_{\mathbf{w}\in\mathcal{W}} F(\mathbf{w})$.

Assume that there are N clients in total and M of them are malicious. The i-th client has a local dataset D_i. The empirical loss of the i-th client is $F_i(\mathbf{w}) = \frac{1}{|D_i|}\sum_{z\in D_i} f(\mathbf{w}; z)$. In the t-th round, the central server randomly samples n clients and distributes the global model $\mathbf{w}_t$ to them. Following existing works [4, 7, 40], we define a benign client will submit update $\mathbf{g}_t^i = \nabla F_i(\mathbf{w}_t)$ and quantity $q_t^i = |D_i|$, while a malicious client can submit an arbitrary update and an arbitrary quantity to the server. After receiving the updates and quantities from the sampled n clients, the server computes the global update with a certain aggregation rule $\mathcal{A}$: $\mathbf{g}_{t+1} = \mathcal{A}(\mathbf{g}_t^1, ..., \mathbf{g}_t^n, q_t^1, ..., q_t^n)$.

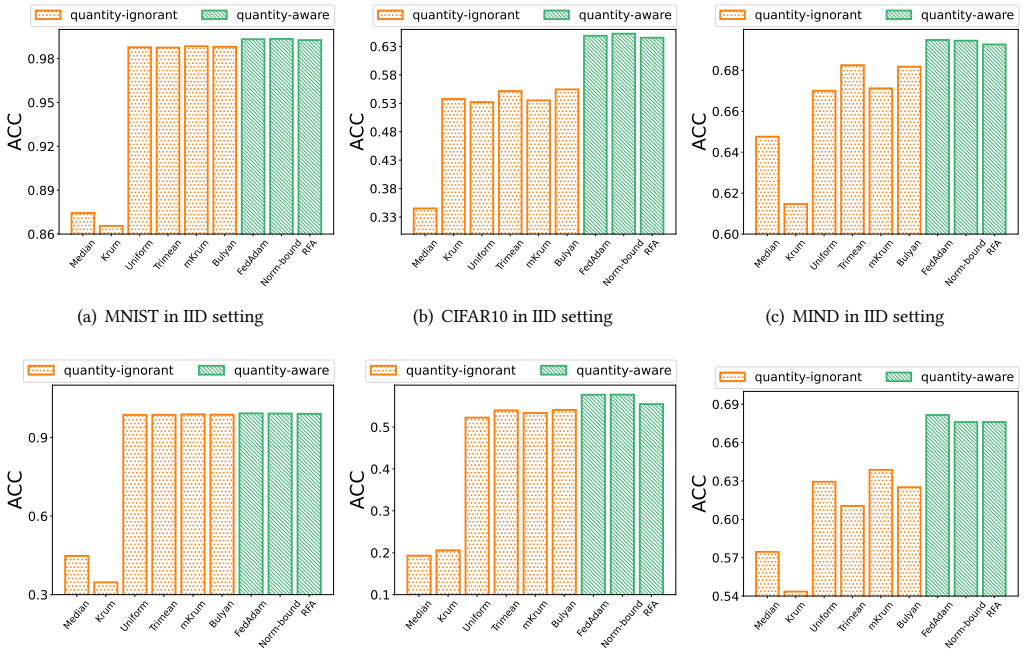

(a) MNIST in IID setting (b) CIFAR10 in IID setting (c) MIND in IID setting

(d) MNIST in non-IID setting (e) CIFAR10 in non-IID setting (f) MIND in non-IID setting

Figure 1: Quantity-aware methods outperform quantity-ignorant methods on three datasets in both IID and non-IID settings.

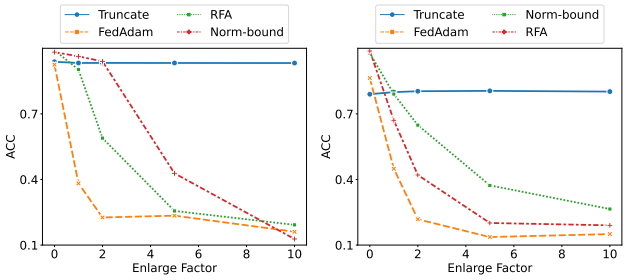

(a) MNIST in fixed-ratio IID setting (b) MNIST in fixed-ratio non-IID setting

Figure 2: Quantity-aware methods are not robust to LIE-based quantity-enhanced attacks.

Some existing robust aggregation algorithms, e.g., mKrum [4], Bulyan [7], and Trimean [40], require estimation of the upper bound of the number of malicious clients, denoted by $\widetilde{m}$, in each round using a fixed parameter for all rounds. However, in cross-device federated learning, due to the large number of clients, only a subset of clients is selected for participation in each round. The number of malicious clients m in each round follows a hypergeometric distribution and is thus hard to be estimated by a fixed parameter. Over-estimating the number of malicious clients leads to some benign clients being filtered out, while underestimating the number of malicious clients may result in some malicious updates being included in the model aggregation. In our work, we consider two settings: fixed-ratio setting and dynamic-ratio setting. In the fixed-ratio setting, the number of malicious clients m in each round is fixed, i.e., $m = \lceil \frac{nM}{N} \rceil$. Since m is not a random variable, estimating m with a fixed parameter is feasible. The fixed-ratio setting, while not representative of real-world cross-device federated learning, provides a baseline for the upper limit of defense performance in filtering out malicious updates. In contrast, the dynamic-ratio setting involves a fixed total number of malicious clients, M, but the exact number of malicious clients per round is unknown, which better reflects real-world federated learning situations.

4 THREAT MODEL

Following existing works [8], in this section, we introduce the objective, knowledge, and capability of attackers and the details of quantity-enhanced attacks.

Attacker's Objective. The attacker's objective is to carry out untargeted attacks on the federated learning system, which aims to degrade the overall performance of the global model on arbitrary input samples.

Attacker's Knowledge. Since the server distributes the global model to clients in each round, the attacker knows the model structure, the local model parameters, and the local training code. Due to the privacy-protecting nature of federal learning, the attacker cannot access the datasets of other clients. Thus, the attacker has partial knowledge of the data distribution. Since the server might not release its aggregation code, the attacker does not know the aggregation rule applied by the server.

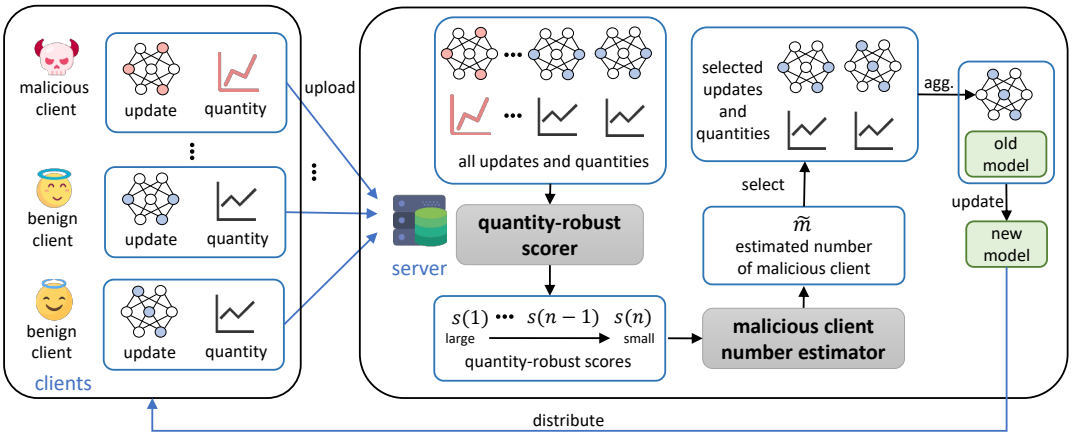

Figure 3: The framework of our FedRA.

Attacker's Capability. Building on prior attack methods [2, 8], we consider the scenario where an attacker controls M malicious clients. These clients can coordinate with each other and use benign data stored on their devices to generate malicious updates and quantities. If any of the malicious clients are selected by the server, they can upload the malicious updates and quantities to the server, degrading the performance of the global model.

Quantity-enhanced Attack. In addition to generating malicious updates via existing untargeted attacks, the attacker also submits large quantities to obtain unfairly high weight in model aggregation, resulting in an amplified impact of malicious updates on the global model. The malicious clients first collaborate to compute the mean and standard deviation of their quantities, which are denoted as μ_q^m and σ_q^m, respectively. The final submitted quantity is defined as $\mu_q^m + \alpha_q \sigma_q^m$, where α_q is the quantity-enlarging factor. α_q should be as large as possible but not detectable by the server

5 EXISTING DEFENSES ARE SUB-OPTIMAL IN QUANTITY-IMBALANCED SCENARIOS

In this section, we prove that both quantity-ignorant and quantity-aware defenses are sub-optimal in quantity-imbalanced scenarios. To simulate quantity-imbalanced settings, we make the quantities of the benign client datasets obey log-normal distributions, which is a typical common long-tailed distribution in real-world scenarios [6, 11, 16, 20, 23]. The detailed experimental settings are in Section 8.

5.1 Quantity-ignorant Methods

In this subsection, we compare the performance of quantity-ignorant methods (Krum, mKrum, Median, TriMean, Bulyan, and Uniform) with that of quantity-aware methods (FedAdam, Norm-bounding, and RFA) in both IID and non-IID non-attack settings. The experimental results on MNIST, CIFAR10, and MIND are shown in Figure 1. We can observe that the performance of quantity-ignorant methods is consistently lower than that of quantity-aware methods. This is because the expectation of the local model error decreases as the sample size of the training dataset increases [31]. Assigning higher weight to the local models trained with larger datasets reduced the aggregation error of the global model.

5.2 Quantity-aware Methods

In this subsection, we analyze the performance of quantity-aware methods (FedAdam, Norm-bounding, and RFA) in IID fixed-ratio settings when exposed to quantity-enhanced attacks. We set the quantity-enlarging factor $\alpha_q \in \{0, 1, 2, 5, 10\}$. Due to the space limitation, we show the results of LIE-based quantity-enhanced attacks on MNIST datasets in Figure 2. We can observe that the performance of quantity-aware methods degrades as the quantity-enlarging factor α_q increases. This is because these methods by default treat the quantities submitted by clients as benign, which is vulnerable to quantity-enhanced attacks since the large quantities can amplify the impact of malicious updates.

We also show the performance of Truncate in Figure 2. We can observe that its performance is stable but sub-optimal under the quantity-enhanced attack. This is because although Truncate limits the upper bound of malicious quantities, it also clips the quantities of benign clients. Additionally, the separate handling of malicious quantities and updates restricts Truncate's ability to effectively filter malicious updates.

6 METHODOLOGY

In this section, we introduce the details of our robust quantity-aware aggregation, named FedRA, which aims to be quantity-robust and achieve optimal performance. It contains two core components, i.e. a quantity-robust scorer and a malicious client number estimator. The quantity-robust scorer calculates scores for clients based on their uploaded updates and quantities. The malicious client number estimator dynamically determines the number of malicious clients in each round, which is more suitable for the dynamic-ratio setting. The framework of our FedRA is shown in Figure 3.

6.1 Quantity-robust Scorer

Lemma 1. *Let $\boldsymbol{g}^i$ and $\boldsymbol{g}^j$ be any pair of independently distributed benign updates and q^i and q^j be the corresponding quantities. If Assumptions 1 and 4 hold, we then have*

$$\mathbb{E}\left[||\boldsymbol{g}^i - \boldsymbol{g}^j||_1\right] \leq \sqrt{2\ln 2}\sqrt{\frac{q^i + q^j}{q^i q^j}}||\boldsymbol{\sigma}||_1, \tag{1}$$

Algorithm 1: FedRA

Server initializes $\mathbf{w}_0$ randomly;
for *each round* $t = 0, ..., T$ **do**
  Randomly select a client set C_t from N clients;
  Distribute the global model $\mathbf{w}_t$ to selected clients;
  for *client* $i \in C_t$ **do**
    $\mathbf{g}_t^i, q_t^i \leftarrow$ **ClientUpdate**$(i, \mathbf{w}_t)$;
    Upload local updates $\mathbf{g}_t^i$ and quantity q_t^i to server;
  end
  // Quantity-robust scorer
  $\mathcal{S} \leftarrow \emptyset, \widetilde{m} \leftarrow \lceil \frac{n\widetilde{M}}{N} \rceil$;
  for $i = 0, 1, ..., n$ **do**
    $s(i) \leftarrow (q_t^i)^\gamma \sum_{i \to j} \sqrt{\frac{q_t^i q_t^j}{q_t^i + q_t^j}} ||\mathbf{g}_t^i - \mathbf{g}_t^j||_1$;
    $\mathcal{S} \leftarrow \mathcal{S} \cup \{s(i)\}$;
  end
  Compute the number of clients c to select;

$$c \leftarrow \begin{cases} n - \widetilde{m} - 1 & \text{fixed-ratio,} \\ n - \textbf{MCNE}(n, \mathcal{S}) & \text{dynamic-ratio.} \end{cases}$$

  Selects c clients C with smallest scores in $\mathcal{S}$;
  $\mathbf{g}_t \leftarrow \frac{1}{\sum_{i \in C} q_t^i} \sum_{i \in C} q_t^i \mathbf{g}_t^i, \mathbf{w}_t = \textbf{Adam}(\mathbf{g}_t)$;
end
// Malicious client number estimator
MCNE$(n, \mathcal{S})$**:**
  $\mathcal{L} \leftarrow \emptyset$;
  for $i = 0, 1, ..., n$ **do**
    Estimate $\mu_b, \sigma_b, \mu_m, \sigma_m$ by Eq 5;
    Compute log-likelihood $\hat{l}(i)$ through Eq 4;
    $\mathcal{L} \leftarrow \mathcal{L} \cup \{\hat{l}(i)\}$;
  end
  $\widetilde{m} \leftarrow \arg\max_{\widetilde{m}} \mathcal{L}$;
  return $\widetilde{m}$;

where $\boldsymbol{\sigma} = [\sigma_1, ...\sigma_d]$, σ_k *is the standard deviation of the k-th dimension of update on the training sample distribution* $\mathcal{D}$*, and* d *is the dimension of* $\mathbf{g}^j$.

Lemma 1 is proved in Appendix A.3, which reflects that the distance between two benign updates varies according to their quantities. If the quantities of two clients are larger, the distance between their updates should be smaller. Inspired by this observation, we design a quantity-robust score, which aims to filter malicious clients considering both their updates and quantities. The quantity-robust score of the i-th client $s(i)$ is defined as follows

$$s(i) = (q^i)^\gamma \sum_{j:i \to j} Q(i,j),\ Q(i,j) = \sqrt{\frac{q^i q^j}{q^i + q^j}} ||\mathbf{g}^i - \mathbf{g}^j||_1, \quad (2)$$

where $i \to j$ denotes that $\mathbf{g}^j$ belongs to the $(n - \widetilde{m} - 2)$ updates closest to $\mathbf{g}^i$ in terms of the Q value, $\widetilde{m}$ is the estimated number of malicious client, $\gamma \leqslant 0.5$ is a hyper-parameter. A smaller quantity-robust score indicates the client is more likely to be benign.

6.2 Malicious Client Number Estimator

Then we need to determine the number of clients to select in each round, which is denoted as c. In the fixed-ratio setting, we can set $c = n - \widetilde{m} - 1 = n - \lceil \frac{n\widetilde{M}}{N} \rceil - 1$, where $\widetilde{m}$ is the estimated number of malicious clients in each round and $\widetilde{M}$ is the estimated number of overall malicious clients. However, in the dynamic-ratio setting, the number of malicious clients varies in each round. Over-estimating $\widetilde{m}$ may result in filtering some benign clients, while underestimating $\widetilde{m}$ may include some malicious updates in the model aggregation. Therefore, we propose a malicious client number estimator to predict the number of malicious clients in each round. We treat $\widetilde{m}$ as a parameter of the distribution of quantity-robust scores, and compute the number of malicious clients $\widetilde{m}$ by maximizing the log-likelihood as follows:

$$\widetilde{m} = \arg\max_{\widetilde{m}} [\ln p(\widetilde{m}, s(1), ..., s(n))] \quad (3)$$

Inspired by Reynolds et al. [29], we assume the quantity-robust scores are independent and follow two Gaussian distributions. Meanwhile, as shown in Appendix B.1, the scores of malicious clients are larger than those of benign clients. Therefore, we further assume the scores can be separated into two groups by a threshold. The group of larger scores belongs to malicious clients and follows one of the Gaussian distributions $\mathcal{N}(\mu_m, \sigma_m)$. The group of the smaller scores belongs to benign clients and follows another Gaussian distribution $\mathcal{N}(\mu_b, \sigma_b)$. We first sort the scores by ascending order, i.e., $s(i) < s(j), \forall i < j$. Since m follows the hypergeometric distribution $\mathcal{H}(n, M, N)$, we can compute $\widetilde{m}$ as follows:

$$\begin{aligned} \widetilde{m} &= \arg\max_{\widetilde{m}} [\ln p(\widetilde{m}) + \sum_{i=1}^{n} \ln p(s(i)|\widetilde{m})] \\ &= \arg\max_{\widetilde{m}} [\ln \tbinom{\widetilde{M}}{\widetilde{m}} \tbinom{N-\widetilde{M}}{n-\widetilde{m}} - (n - \widetilde{m}) \ln \sigma_b - \widetilde{m} \ln \sigma_m \\ &\quad - \sum_{i=1}^{n-\widetilde{m}} \frac{(s(i) - \mu_b)^2}{2\sigma_b^2} - \sum_{i=n-\widetilde{m}+1}^{n} \frac{(s(i) - \mu_m)^2}{2\sigma_m^2}]. \end{aligned} \quad (4)$$

The mean and variance of the two Gaussian distributions are estimated as follows:

$$\begin{aligned} \mu_b &= \frac{1}{n - \widetilde{m}} \sum_{i=1}^{n-\widetilde{m}} s(i), \sigma_b^2 = \frac{1}{n - \widetilde{m} - 1} \sum_{i=1}^{n-\widetilde{m}} (s(i) - \mu_b)^2 \\ \mu_m &= \frac{1}{\widetilde{m}} \sum_{i=n-\widetilde{m}+1}^{n} s(i), \sigma_m^2 = \frac{1}{\widetilde{m} - 1} \sum_{i=n-\widetilde{m}+1}^{n} (s(i) - \mu_m)^2. \end{aligned} \quad (5)$$

One may ask how $s(i)$ is computed since it is relevant with $\widetilde{m}$. A reasonable way is to initialize $\widetilde{m} = \lceil \frac{n\widetilde{M}}{N} \rceil$, iteratively compute $s(i)$ and run the malicious client number estimator to update $\widetilde{m}$. However, our experiments indicate that the performance without iterative approximation is already great enough.

The complete algorithm of our FedRA is shown in Algorithm 1.

7 THEORETICAL ANALYSIS

7.1 Definitions and Assumptions

In this subsection, we introduce some definitions and assumptions used in our theoretical analysis.

Definition 1. (Sub-exponential random variable). A random variable X with $\mathbb{E}[X] = \mu$ is called sub-exponential with parameters (v^2, α) if $\mathbb{E}[e^{\lambda(X-\mu)}] \leq e^{\frac{1}{2}v^2\lambda^2}, \forall|\lambda| < \frac{1}{\alpha}$.

Definition 2. (Lipschitz). h is L-Lipschitz if $|h(\mathbf{w}) - h(\mathbf{w}')| \leq L||\mathbf{w} - \mathbf{w}'||_2, \forall\ \mathbf{w}, \mathbf{w}'$.

Definition 3. (Smoothness). h is L-smooth if $||\nabla h(\mathbf{w}) - \nabla h(\mathbf{w}')|| \leq L||\mathbf{w} - \mathbf{w}'||_2, \forall\ \mathbf{w}, \mathbf{w}'$.

Assumption 1. *(Sub-exponential updates). For all $\boldsymbol{w} \in \mathcal{W}$, the partial derivative of $f(\cdot; z)$ with respect to the k-th dimension of its first argument, denoted as $\partial_k f(\boldsymbol{w}; z)$, is sub-exponential with parameters (v_k^2, α_k) where $\mathrm{Var}_{z\sim\mathcal{D}}[\partial_k f(\boldsymbol{w}; z)] = \sigma_k^2, v_k = \sigma_k, \alpha_k < \frac{\sigma_k}{\sqrt{2\ln 2n}}$, $k \leq d$ and d is the dimension of $\boldsymbol{w}$.*

Assumption 2. *(Smoothness of F). The population loss function $F(\cdot)$ is L_F-smooth.*

Assumption 3. *(Minimizer in $\mathcal{W}$). Let $\boldsymbol{w}^* = \arg\min_{\boldsymbol{w}\in\mathcal{W}} F(\boldsymbol{w})$. We assume that $\nabla F(\boldsymbol{w}^*) = 0$.*

Assumption 4. *(Independent identical distribution). For any benign client i, $z \in D_i$ are independently sampled from $\mathcal{D}$.*

Assumptions 1, 2, 3 and 4 have been applied in previous works [4, 7, 40]. Then we introduce the definition of quantity-robust.

Lemma 2. *For any benign update $\boldsymbol{g}^i$ and quantity q^i, when Assumptions 1 and 4 hold, we have*

$$\mathbb{E}[\sqrt{q^i}||\boldsymbol{g}^i - \boldsymbol{\mu}||_1] \leq \sqrt{2\ln 2}||\boldsymbol{\sigma}||_1, \tag{6}$$

where $\boldsymbol{\sigma} = [\sigma_1, ...\sigma_d]$, $\mathbb{E}_{z\sim\mathcal{D}}[\nabla f(\boldsymbol{w}; z)] = \boldsymbol{\mu}$.

Lemma 2 is proved in Appendix A.4, which shows the quantity-aware error of benign updates $\mathbb{E}[\sqrt{q^i}||\boldsymbol{g}^i - \boldsymbol{\mu}||_1]$ is constant. It inspires us to prove whether a method is quantity-robust by proving the quantity-aware error of every selected update is irrelevant to malicious quantities. The formulation of the quantity-robust definition is as follows:

Definition 4. (Quantity-robust). An aggregation rule is quantity-robust, only when every selected update $\mathbf{g}$ and quantity q satisfies $\mathbb{E}[\sqrt{q}||\mathbf{g} - \boldsymbol{\mu}||_1] \leq C$, where C is irrelevant to malicious quantities and updates.

7.2 FedRA is Quantity-robust

Proposition 1. *Let $\boldsymbol{g}^1, ..., \boldsymbol{g}^{n-m}$ be independent benign updates with quantities $q^1, ..., q^{n-m}$, where $\boldsymbol{g}^i \in \mathbb{R}^d$, and $\mathbb{E}[\boldsymbol{g}^i] = \boldsymbol{\mu}$. Let $\boldsymbol{g}^{n-m+1}, ..., \boldsymbol{g}^n$ be malicious updates in $\mathbb{R}^d$ and $q^{n-m+1}, ..., q^n$ be their quantities. Suppose that Assumptions 1 and 4 hold for all benign updates. If $2m + 2 \leqslant n$, $\gamma = 0.5$, then FedRA satisfies*

$$\mathbb{E}[\sqrt{q}||\boldsymbol{g} - \overline{\boldsymbol{g}}||_1] \leqslant A_{n,m}B_q||\boldsymbol{\sigma}||_1, \tag{7}$$

Table 1: Dataset statistics.

Dataset	#Classes	#Train	#Test	#Clients	#Train per client		
					Mean	Std	Max
MNIST	10	60,000	10,000	3,025	19.77	179.28	6,820
CIFAR10	10	50,000	10,000	3,115	16.05	200.14	8,933
MIND	18	71,068	20,307	2,880	24.68	299.61	9,398

where $\boldsymbol{g}$ and q is the quantity and update of the client with the smallest quantity-robust score,

$$\begin{aligned} A_{n,m} &= \sqrt{2\ln 2}(n-m) + m\sqrt{2\ln 2(n-m)}, \\ B_q &= \frac{\max_{benign\ i}[q^i + 1]\min_{benign\ i}}{\sum_{i\in\mathcal{B}} q^i}, \\ \overline{\boldsymbol{g}} &= \frac{1}{\sum\limits_{\substack{j:i_*\to j \\ benign\ j}} q^j} \sum_{\substack{j:i_*\to j \\ benign\ j}} q^j \boldsymbol{g}^j, \end{aligned} \tag{8}$$

$\mathcal{B}$ is denoted as the (n-m-2) benign clients with smallest quantities. If $\max\limits_{malicious\ i} q^i < \sum\limits_{i\in\mathcal{B}} q^i$, then $\boldsymbol{g}$ satisfies

$$\mathbb{E}[\sqrt{q}||\boldsymbol{g} - \boldsymbol{\mu}||_1] \leqslant (A_{n,m}B_q + C_{n,m})||\boldsymbol{\sigma}||_1, \tag{9}$$

where $C_{n,m} = \sqrt{2\ln 2(n-m)} + \sqrt{2\ln 2}$.

Remark 1. *Proposition 1 can be extended to other selected updates and quantities with larger B_q irrelevant to malicious quantities and smaller benign client set $\mathcal{B}$.*

Proposition 1 is proved in Appendix A.1. Since the error of FedRA is controlled by $A_{n,m}$, B_q, $||\boldsymbol{\sigma}||_1$, and $C_{n,m}$ which are irrelevant to malicious quantities and updates, FedRA is quantity-robust.

We state the statistical error guarantees of FedRA for smooth non-convex F.

Theorem 5. *Assume that Assumptions 1, 2 3 and 4 hold, $2m+2 < n$, $\gamma = 0.5$ and $\max\limits_{malicious\ i} q^i < \sum\limits_{i\in\mathcal{B}} q^i$. Choose $\eta = 1/L_F$. If $\boldsymbol{w}_{t+1} = \boldsymbol{w}_t - \eta\boldsymbol{g}_t$, after T iterations with FedRA, we have*

$$\begin{aligned} \min_{t=0,...,T} \mathbb{E}[||\nabla F(\boldsymbol{w}_t)||_2^2] \leq\ & \frac{2L_F}{T}\mathbb{E}[F(\boldsymbol{w}_0) - F(\boldsymbol{w}^*)] \\ & + \frac{1}{T}\sum_{t=0}^{T-1}((A_{n,m}B_q + C_{n,m})||\boldsymbol{\sigma}||_1)^2. \end{aligned} \tag{10}$$

Theorem 5 is proved in Appendix A.2.

8 EXPERIMENTS

8.1 Datasets and Experimental Settings

Dataset. We conduct experiments on three public datasets:, i.e., MNIST [14], CIFAR10 [12], and MIND [35]. The quantities follow a long-tailed distribution, i.e., log-normal distribution. The average sample size of clients is around 20, and the σ of the log-normal distribution is 3. We randomly shuffle the dataset and partition it according to the quantities. For the IID setting, we randomly divide the dataset into clients' local datasets. For the non-IID setting, we guarantee the local datasets of most clients contain only one class. The detailed statistics of the datasets are shown in Table 1.

Table 2: Performance of different methods in IID fixed-ratio settings, with the best results in bold and second-best ones in underlined. *Best QI refers to the best quantity-ignorant method.

Dataset	Method	Label Flip					LIE					Optimize				
		0	1	2	5	10	0	1	2	5	10	0	1	2	5	10
MNIST	Best QI*	98.77	98.77	98.77	98.77	98.77	94.50	94.50	94.50	94.50	94.50	98.76	98.76	98.76	98.76	98.76
	FedAdam	98.68	97.77	97.05	94.42	90.38	92.52	38.23	22.63	23.45	16.09	9.82	9.46	8.92	8.92	8.92
	Norm-Bound	99.08	98.65	98.33	97.47	96.09	98.25	96.31	94.02	42.81	12.78	97.59	97.57	95.80	8.92	8.92
	RFA	**99.31**	99.11	98.78	98.36	97.59	99.05	90.28	58.91	25.61	19.24	97.77	10.68	8.92	8.92	8.92
	Truncate	97.20	97.19	97.18	97.16	97.17	93.83	93.28	93.31	93.28	93.25	52.87	52.44	56.61	53.27	55.22
	FedRA	99.30	**99.25**	**99.30**	**99.25**	**99.31**	**99.20**	**99.16**	**99.21**	**99.08**	**99.20**	**99.21**	**99.27**	**99.22**	**99.25**	**99.26**
CIFAR10	Best QI*	51.42	51.42	51.42	51.42	51.42	50.65	50.65	50.65	50.65	50.65	52.60	52.60	52.60	52.60	52.60
	FedAdam	56.95	38.60	31.32	19.35	15.02	13.43	10.12	10.18	10.01	10.00	12.64	10.00	10.00	10.00	10.00
	Norm-Bound	60.22	43.81	35.44	27.44	17.54	20.27	13.61	10.62	13.74	12.21	25.13	10.00	10.00	10.00	10.00
	RFA	**62.19**	52.11	46.01	36.86	29.34	19.62	10.03	10.01	10.00	10.08	12.87	10.00	10.00	10.00	10.00
	Truncate	47.45	45.81	45.57	45.57	45.57	13.46	14.23	11.25	11.25	11.25	12.68	12.37	12.41	12.41	12.41
	FedRA	60.44	**61.73**	**62.11**	**62.28**	**62.37**	**62.58**	**62.58**	**62.58**	**62.58**	**62.58**	**62.69**	**62.69**	**62.69**	**62.69**	**62.69**
MIND	Best QI*	66.52	66.52	66.52	66.52	66.52	61.19	61.19	61.19	61.19	61.19	67.25	67.25	67.25	67.25	67.25
	FedAdam	67.03	63.35	62.03	60.91	59.01	53.69	31.84	31.84	4.83	4.83	28.70	10.73	9.77	8.26	8.39
	Norm-Bound	67.66	63.30	62.19	61.02	59.35	54.41	31.84	31.84	4.83	4.83	54.88	23.35	7.52	6.90	6.97
	RFA	**70.30**	66.49	65.47	63.76	61.34	64.52	31.84	31.84	31.84	4.83	50.37	9.04	6.35	5.45	4.98
	Truncate	67.92	67.68	67.68	67.68	67.68	53.64	52.70	52.70	53.11	53.11	54.76	54.59	54.59	54.59	54.59
	FedRA	69.96	**69.61**	**69.94**	**70.15**	**70.27**	**70.71**	**70.73**	**70.70**	**70.70**	**70.70**	**70.85**	**70.85**	**70.85**	**70.85**	**70.85**

Table 3: Performance of quantity-ignorant methods in IID fixed-ratio settings.

Dataset	Attack	Krum	Median	Trimean	mKrum	Bulyan
MNIST	Label Flip	87.01	88.62	96.93	98.77	96.89
	LIE	84.11	85.24	91.55	89.51	94.50
	Optimize	87.04	46.35	30.34	98.76	96.92
CIFAR10	Label Flip	51.42	27.85	49.39	50.37	47.18
	LIE	50.65	18.53	15.55	22.68	24.58
	Optimize	52.60	19.04	18.77	51.69	51.48
MIND	Label Flip	64.40	56.85	65.11	65.54	66.52
	LIE	61.19	55.37	54.39	56.25	59.57
	Optimize	62.53	54.10	38.94	67.25	67.11

Configurations. In our experiments, we use CNN networks as base models for the MNIST and CIFAR10 datasets. For the MIND dataset, we use a Text-CNN as the base model, and initialize the word embedding matrix with pre-trained Glove embeddings [24]. We apply FedAdam [28] to accelerate model convergence in all methods. We apply dropout with dropout rate 0.2 to mitigate overfitting. The learning rate is 0.001 for CIFAR10, and 0.0001 for MNIST and MIND. The maximum of training rounds is 10,000 for MNIST and CIFAR10, and 15,000 for MIND. The ratio of malicious clients M/N is 0.1. The number of clients sampled in each round n is 50. γ is 0.1. The server estimates $\widetilde{M}$ as M.

Baselines. We compare our FedRA with several baseline methods, including 1) **Median** [40], applying coordinate-wise median on each dimension of updates; 2) **Trimean** [40], applying coordinate-wise trimmed-mean on each dimension of updates; 3) **Krum** [4], selecting the update that is closest to a subset of neighboring updates based on the square distance; 4) **mKrum** [4], a variance of Krum that selects multiple updates and averages the selected updates; 5) **Bulyan** [7], selecting multiple clients with mKrum and aggregating the selected updates with Trimean; 6) **Norm-bounding** [33], clipping the L_2 norm of each update with a certain threshold; 7) **RFA** [25], applying an approximation algorithm to minimize the geometric median of updates; 8) **Truncate** [26], limiting the quantity of each client under a dynamic threshold in each round and applying quantity-aware Trimean.

Attack Model. We suppose an attacker controls malicious clients. Each malicious client, if sampled, submits malicious updates and a malicious quantity. We implement three existing untargeted poisoning attack methods to create malicious updates, including 1) **Label Flip** [8]: a data poisoning attack that manipulates labels of training samples; 2) **LIE** [2]: adding small enough noise in the mean of benign updates to circumvent defenses; 3) **Optimize** [8]: a model poisoning attack that adds noise in the opposite position of benign updates. To create malicious quantities, we set the malicious quantity $\alpha_q \in \{0, 1, 2, 5, 10\}$. It is noted that when α_q equals or is less than 10, the malicious quantity is still smaller than the maximum benign quantity in training dataset. Therefore, the malicious quantity is in a reasonable range in our settings.

8.2 Performance in IID Fixed-ratio Setting

In this subsection, we conduct experiments in the fixed-ratio setting to analyze the effectiveness of our quantity-robust scorer. The experimental results are shown in Table 2 and Table 3. We can make the following observations from the tables. First, our FedRA outperforms the best quantity-ignorant defense in the fixed-ratio settings in the vast majority of cases. This is because our method performs weighted averaging on selected updates based on their quantities. Second, our FedRA has stable performance with different quantity-enlarging factors and outperforms other quantity-aware methods. This is because FedRA can defend against quantity-enhanced attacks by jointly considering updates and quantities to filter malicious clients. These two observations reflect the effectiveness of our FedRA algorithm. Third, the performance of quantity-aware defenses, i.e., RFA and Norm-bound, becomes worse with larger

Table 4: Performance of different methods in IID dynamic-ratio settings, with the best results in bold and second-best ones in underlined. *Best QI refers to the best quantity-ignorant method.

Dataset	Method	Label Flip					LIE					Optimize				
		0	1	2	5	10	0	1	2	5	10	0	1	2	5	10
MNIST	Best QI	98.65	98.65	98.65	**98.65**	98.65	93.16	93.16	93.16	93.16	93.16	97.11	97.11	97.11	97.11	97.11
	FedAdam	98.74	97.84	97.17	95.21	92.89	93.25	50.42	24.25	16.69	16.26	9.69	9.67	8.92	8.92	8.92
	Norm-Bound	99.09	98.75	98.51	97.76	96.56	98.35	96.49	94.32	76.15	19.67	97.76	97.56	96.29	8.92	8.92
	RFA	**99.31**	**99.08**	**98.79**	98.38	97.54	98.70	91.21	64.81	28.63	18.72	96.32	9.79	8.92	8.92	8.92
	Truncate	97.23	97.00	96.98	96.92	96.93	84.71	76.88	74.34	73.15	72.85	9.92	9.78	9.78	9.97	10.02
	FedRA	98.53	98.46	98.48	98.49	**98.66**	**99.27**	**99.32**	**99.30**	**99.31**	**99.28**	**98.87**	**98.95**	**98.93**	**98.81**	**98.90**
CIFAR10	Best QI	51.75	51.75	51.75	51.75	51.75	52.14	52.14	52.14	52.14	52.14	52.85	52.85	52.85	52.85	52.85
	FedAdam	56.30	40.93	34.89	22.43	15.86	13.61	10.68	10.40	10.00	10.32	11.76	10.00	10.00	10.00	10.00
	Norm-Bound	60.14	45.25	38.83	27.02	19.41	22.95	13.58	11.20	10.59	13.59	26.79	10.00	10.00	10.00	10.00
	RFA	62.31	50.36	45.98	33.32	22.42	18.56	10.01	10.16	10.02	10.10	15.90	10.00	10.00	10.00	10.00
	Truncate	48.01	41.82	45.28	45.05	44.11	14.38	13.49	13.76	13.71	13.62	13.89	10.67	12.17	13.42	12.94
	FedRA	**61.86**	**61.32**	**62.68**	**62.59**	**63.92**	**64.58**	**64.80**	**64.53**	**64.22**	**64.23**	**64.32**	**64.64**	**64.26**	**64.45**	**64.21**
MIND	Best QI	66.46	66.46	66.46	66.46	66.46	59.09	59.09	59.09	59.09	59.09	66.50	66.50	66.50	66.50	66.50
	FedAdam	65.32	63.23	61.34	60.96	59.16	53.74	31.84	31.79	31.84	4.83	17.53	12.12	10.04	9.53	8.82
	Norm-Bound	66.13	63.54	61.24	60.61	58.99	54.18	31.84	20.02	31.84	4.83	55.65	11.92	8.04	5.97	5.57
	RFA	67.53	65.57	65.31	62.12	59.81	61.69	31.82	31.84	31.84	31.84	41.09	8.90	6.03	6.50	1.74
	Truncate	68.49	67.93	67.83	67.90	67.84	51.94	46.68	46.57	46.52	46.51	23.64	17.16	17.32	17.47	17.47
	FedRA	**69.96**	**69.92**	**69.97**	**70.11**	**70.49**	**71.09**	**71.12**	**71.11**	**71.11**	**71.11**	**71.02**	**70.89**	**71.05**	**71.13**	**71.12**

Table 5: Performance of quantity-ignorant methods in IID dynamic-ratio settings.

Dataset	Attack	Krum	Median	Trimean	mKrum	Bulyan
MNIST	Label Flip	87.67	87.90	96.86	98.65	97.30
	LIE	83.03	87.05	79.44	93.16	79.08
	Optimize	86.03	44.92	10.70	97.11	96.59
CIFAR10	Label Flip	51.75	33.25	49.39	51.71	49.61
	LIE	52.14	18.23	13.31	21.44	17.63
	Optimize	52.56	12.63	16.60	52.85	52.16
MIND	Label Flip	61.92	56.38	65.31	65.62	66.46
	LIE	59.09	55.15	54.11	57.46	55.38
	Optimize	62.81	54.12	38.18	65.37	66.50

quantity-enlarging factors. This is because these quantity-aware defenses by default treat received quantities as benign, which is vulnerable to quantity-enhanced attacks. Finally, Truncate has stable performance with different quantity-enlarging factors, but its performance is lower than FedRA. This is because the Truncate algorithm is quantity-robust by limiting quantities submitted by malicious clients. However, it also restricts quantities of benign clients. Meanwhile, it does not filter malicious clients by jointly considering quantities and updates. Thus, it has sub-optimal performance.

8.3 Performance in IID Dynamic-ratio Setting

In this subsection, we conduct experiments in the IID dynamic-ratio setting to analyze the effectiveness of our malicious client number selector. The experimental results are shown in Table 4 and Table 5. Besides the same observations in the fixed-ratio setting, we can make several additional observations. First, our FedRA has stable performance with different quantity-enlarging factors. It outperforms or has similar performance as the best quantity-ignorant defense. This shows the effectiveness of our FedRA with the malicious client estimator. Second, the algorithms that need to estimate the number or the upper bound of malicious clients, i.e., mKrum, Trimean, Bulyan, and Truncate, have lower performance in the dynamic-ratio setting than in the fixed-ratio setting. This is because the number of malicious clients in each round changes dynamically. Over-estimating makes a subset of benign clients excluded, while under-estimating causes some malicious clients selected in some rounds.

8.4 Performance in non-IID Setting

In this subsection, we analyze the performance of our FedRA in the non-IID dynamic-ratio setting. The experimental results are shown in Table 6 and Table 7, where we can have several observations. First, our FedRA consistently outperforms both quantity-ignorant and quantity-aware methods under LIE-based and Optimize-based quantity-enhanced attacks. This is because we apply quantity-robust scorer which helps accurately filter out malicious clients and effectively aggregate updates with quantities. Second, the performance of our FedRA drops under Label-flip-based attacks. Suppose the sample sizes of all classes are the same. If a benign client has a large dataset with a single class, then it is likely there are fewer benign clients holding the dataset with the same class since in the non-IID settings most clients only have datasets with a single class. Therefore, benign clients with large quantities are likely to be filtered out, especially under less advanced attacks like Label flip. Finally, compared to the performance under IID settings, the performance of all methods under non-IID settings drops. This is because the non-IID settings introduce a drift in local updates, leading to slow model convergence [10, 18]. Meanwhile, in non-IID settings the variance of clients' local updates becomes larger, giving malicious updates more chances to circumvent defenses.

8.5 Ablation Study

In this subsection, we compare applying the malicious client number estimator (MCNE) with under-estimating and over-estimating

Table 6: Performance of different methods in non–IID dynamic-ratio settings, with the best results in bold and second-best ones in underlined. *Best QI refers to the best quantity-ignorant method.

Dataset	Method	Label Flip					LIE					Optimize				
		0	1	2	5	10	0	1	2	5	10	0	1	2	5	10
MNIST	Best QI	98.49	98.49	98.49	**98.49**	**98.49**	89.87	89.87	89.87	89.87	89.87	96.94	96.94	96.94	96.94	96.94
	FedAdam	98.67	97.55	96.78	93.42	87.58	90.59	44.44	28.09	15.30	19.13	10.36	11.39	11.35	11.35	11.35
	Norm-Bound	**99.03**	98.69	98.54	97.86	95.81	97.61	83.45	69.37	36.57	19.98	95.92	85.61	63.39	11.35	11.35
	RFA	98.99	**98.93**	**98.54**	97.89	95.78	98.46	72.32	53.56	26.02	19.46	95.62	8.56	11.63	11.35	11.35
	Truncate	88.88	87.76	86.95	87.29	87.28	51.37	45.40	45.24	44.57	44.93	11.24	13.05	13.32	13.34	13.34
	FedRA	95.28	95.68	95.16	95.65	95.31	**99.00**	**99.03**	**99.04**	**99.05**	**99.04**	**98.48**	**98.47**	**98.49**	**98.58**	**98.60**
CIFAR10	Best QI	49.88	**49.88**	**49.88**	**49.88**	**49.88**	20.18	20.18	20.18	20.18	20.18	40.90	40.90	40.90	40.90	40.90
	FedAdam	50.70	34.62	29.33	17.06	14.20	14.07	10.24	10.17	10.01	10.06	14.97	10.00	10.00	10.00	10.00
	Norm-Bound	**53.58**	37.97	31.03	22.97	16.58	14.34	10.65	10.69	11.74	10.54	17.10	10.00	10.00	10.00	10.00
	RFA	51.59	38.11	30.00	21.10	17.89	13.86	10.00	10.05	10.06	10.01	14.17	10.00	10.00	10.00	10.00
	Truncate	22.67	25.16	26.91	24.92	23.99	13.97	13.74	13.77	14.41	13.98	13.50	10.96	10.08	11.42	12.88
	FedRA	44.29	45.90	45.57	47.93	49.69	**59.48**	**59.45**	**59.49**	**59.04**	**59.36**	**59.01**	**58.92**	**59.25**	**58.38**	**58.42**
MIND	Best QI	62.59	62.59	62.59	62.59	62.59	59.65	59.65	59.65	59.65	59.65	60.06	60.06	60.06	60.06	60.06
	FedAdam	63.60	62.01	60.93	57.63	55.19	54.96	31.84	4.52	4.52	4.52	26.93	13.81	11.48	7.66	1.74
	Norm-Bound	65.92	62.91	60.79	58.64	56.36	54.81	31.84	31.84	31.84	31.84	4.61	17.36	14.00	5.96	1.36
	RFA	**68.10**	65.37	61.86	55.88	55.62	56.53	31.84	31.84	31.84	4.52	46.73	15.49	8.94	1.53	0.96
	Truncate	62.46	61.59	62.04	61.52	61.57	31.84	31.84	31.84	31.93	29.65	29.64	25.50	26.22	21.31	24.47
	FedRA	66.33	**67.07**	**66.30**	**67.02**	**66.86**	**69.20**	**69.17**	**69.22**	**69.25**	**69.21**	**69.20**	**69.22**	**69.04**	**69.16**	**69.17**

Table 7: Performance of quantity-ignorant methods in non-IID dynamic-ratio settings.

Dataset	Attack	Krum	Median	Trimean	mKrum	Bulyan
MNIST	Label Flip	36.71	39.25	88.13	98.49	93.90
	LIE	36.12	33.62	50.93	89.87	47.63
	Optimize	35.36	9.67	10.99	96.94	83.17
CIFAR10	Label Flip	21.51	20.15	32.58	49.88	20.68
	LIE	20.18	13.40	13.62	16.64	13.60
	Optimize	21.91	14.81	13.27	40.90	25.22
MIND	Label Flip	50.89	56.04	59.93	62.59	60.45
	LIE	54.07	35.32	31.33	46.29	59.65
	Optimize	53.59	17.59	10.11	56.01	60.06

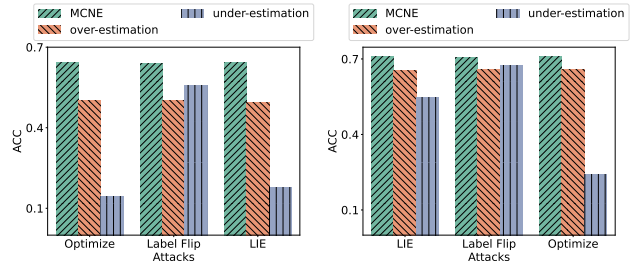

(a) CIFAR10 (b) MIND

Figure 4: Results of applying malicious client number estimator, under-estimating and over-estimating the number of malicious clients in the IID dynamic-ratio setting.

the number of malicious clients $\widetilde{m}$ in the IID dynamic-ratio settings. For the experiments of under-estimation, we set the estimated number of malicious clients $\widetilde{m}$ as 5, which equals the expectation of selected malicious clients in each round. For the experiments of over-estimation, we set the estimated number of malicious clients $\widetilde{m}$ as 15, since $p(m > 15) \leqslant 1.54^{-5}$. Due to the space limitation, we only display the experimental results on CIFAR10 and MIND in Figure 4. The results on MNIST are shown in Appendix C The performance of experiments with MCNE is consistently higher than those with over-estimation and under-estimation. This is because the number of malicious clients follows a hypergeometric distribution in the dynamic-ratio setting, which is hard to be estimated by a fixed parameter. Under-estimating the number of malicious clients makes some malicious clients selected in some rounds, while over-estimation filters some benign clients in most rounds.

9 CONCLUSION

In this paper, we propose FedRA, a robust quantity-aware aggregation method for federated learning. It aims to aggregate clients' local model updates with awareness of clients' quantities to benefit model performance while being quantity-robust to defend against quantity-enhanced attacks. FedRA contains two key components, i.e., quantity-robust scorer and malicious client number estimator. Based on the principle that benign updates with larger quantities should be closer, the quantity-robust scorer assigns malicious updates higher scores jointly considering received model updates and quantities. Since the number of malicious clients varies in different rounds, the malicious client number estimator predicts the number of clients by maximizing the log-likelihood of quantity robust scores. We theoretically prove that our FedRA is quantity-robust. Meanwhile, experiments on three public datasets demonstrate the effectiveness of our FedRA.

REFERENCES

[1] Eugene Bagdasaryan, Andreas Veit, Yiqing Hua, Deborah Estrin, and Vitaly Shmatikov. 2020. How to backdoor federated learning. In *AISTATS*. 2938–2948.
[2] Gilad Baruch, Moran Baruch, and Yoav Goldberg. 2019. A Little Is Enough: Circumventing Defenses For Distributed Learning. In *NIPS*, Vol. 32.

[3] Arjun Nitin Bhagoji, Supriyo Chakraborty, Prateek Mittal, and Seraphin Calo. 2019. Analyzing federated learning through an adversarial lens. In *ICML*. 634–643.

[4] Peva Blanchard, El Mahdi El Mhamdi, Rachid Guerraoui, and Julien Stainer. 2017. Machine learning with adversaries: Byzantine tolerant gradient descent. *NIPS* 30 (2017).

[5] Mingqing Chen, Rajiv Mathews, Tom Ouyang, and Françoise Beaufays. 2019. Federated learning of out-of-vocabulary words. *arXiv preprint arXiv:1903.10635* (2019).

[6] Zhihong Chen, Rong Xiao, Chenliang Li, Gangfeng Ye, Haochuan Sun, and Hongbo Deng. 2020. Esam: Discriminative domain adaptation with non-displayed items to improve long-tail performance. In *SIGIR*. 579–588.

[7] El Mahdi El Mhamdi, Rachid Guerraoui, and Sébastien Rouault. 2018. The Hidden Vulnerability of Distributed Learning in Byzantium. In *ICML*, Vol. 80. 3521–3530.

[8] Minghong Fang, Xiaoyu Cao, Jinyuan Jia, and Neil Zhenqiang Gong. 2020. Local Model Poisoning Attacks to Byzantine-Robust Federated Learning. In *USENIX*.

[9] Andrew Hard, Kanishka Rao, Rajiv Mathews, Swaroop Ramaswamy, Françoise Beaufays, Sean Augenstein, Hubert Eichner, Chloé Kiddon, and Daniel Ramage. 2018. Federated learning for mobile keyboard prediction. *arXiv preprint arXiv:1811.03604* (2018).

[10] Sai Praneeth Karimireddy, Satyen Kale, Mehryar Mohri, Sashank Reddi, Sebastian Stich, and Ananda Theertha Suresh. 2020. Scaffold: Stochastic controlled averaging for federated learning. In *ICML*. 5132–5143.

[11] Yejin Kim, Kwangseob Kim, Chanyoung Park, and Hwanjo Yu. 2019. Sequential and Diverse Recommendation with Long Tail.. In *IJCAI*, Vol. 19. 2740–2746.

[12] Alex Krizhevsky, Geoffrey Hinton, et al. 2009. Learning multiple layers of features from tiny images. (2009).

[13] Yogesh Kumar and Ruchi Singla. 2021. Federated learning systems for healthcare: perspective and recent progress. *Federated Learning Systems: Towards Next-Generation AI* (2021), 141–156.

[14] Yann LeCun, Léon Bottou, Yoshua Bengio, and Patrick Haffner. 1998. Gradient-based learning applied to document recognition. *Proc. IEEE* 86, 11 (1998), 2278–2324.

[15] Jingjing Li, Ke Lu, Zi Huang, and Heng Tao Shen. 2017. Two Birds One Stone: On Both Cold-Start and Long-Tail Recommendation. In *MM*. 898–906.

[16] Jingjing Li, Ke Lu, Zi Huang, and Heng Tao Shen. 2019. On both cold-start and long-tail recommendation with social data. *TKDE* 33, 1 (2019), 194–208.

[17] Li Li, Yuxi Fan, Mike Tse, and Kuo-Yi Lin. 2020. A review of applications in federated learning. *Computers & Industrial Engineering* 149 (2020), 106854.

[18] Tian Li, Anit Kumar Sahu, Manzil Zaheer, Maziar Sanjabi, Ameet Talwalkar, and Virginia Smith. 2020. Federated optimization in heterogeneous networks. *Proceedings of Machine Learning and Systems* 2 (2020), 429–450.

[19] Yingqi Liu, Shiqing Ma, Yousra Aafer, Wen-Chuan Lee, Juan Zhai, Weihang Wang, and Xiangyu Zhang. 2017. Trojaning attack on neural networks. In *NDSS*.

[20] Alexander Long, Wei Yin, Thalaiyasingam Ajanthan, Vu Nguyen, Pulak Purkait, Ravi Garg, Alan Blair, Chunhua Shen, and Anton van den Hengel. 2022. Retrieval augmented classification for long-tail visual recognition. In *CVPR*. 6959–6969.

[21] Brendan McMahan, Eider Moore, Daniel Ramage, Seth Hampson, and Blaise Aguera y Arcas. 2017. Communication-efficient learning of deep networks from decentralized data. In *AISTATS*. 1273–1282.

[22] Dinh C Nguyen, Quoc-Viet Pham, Pubudu N Pathirana, Ming Ding, Aruna Seneviratne, Zihuai Lin, Octavia Dobre, and Won-Joo Hwang. 2022. Federated learning for smart healthcare: A survey. *ACM Computing Surveys (CSUR)* 55, 3 (2022), 1–37.

[23] Yoon-Joo Park and Alexander Tuzhilin. 2008. The long tail of recommender systems and how to leverage it. In *RecSys*. 11–18.

[24] Jeffrey Pennington, Richard Socher, and Christopher D Manning. 2014. Glove: Global vectors for word representation. In *EMNLP*. 1532–1543.

[25] Krishna Pillutla, Sham M Kakade, and Zaid Harchaoui. 2019. Robust aggregation for federated learning. *arXiv preprint arXiv:1912.13445* (2019).

[26] Amit Portnoy, Yoav Tirosh, and Danny Hendler. 2020. Towards Federated Learning With Byzantine-Robust Client Weighting. *arXiv preprint arXiv:2004.04986* (2020).

[27] Swaroop Ramaswamy, Rajiv Mathews, Kanishka Rao, and Françoise Beaufays. 2019. Federated learning for emoji prediction in a mobile keyboard. *arXiv preprint arXiv:1906.04329* (2019).

[28] Sashank J. Reddi, Zachary Charles, Manzil Zaheer, Zachary Garrett, Keith Rush, Jakub Konečný, Sanjiv Kumar, and Hugh Brendan McMahan. 2021. Adaptive Federated Optimization. In *ICLR*.

[29] Douglas A Reynolds et al. 2009. Gaussian mixture models. *Encyclopedia of biometrics* 741, 659-663 (2009).

[30] Nicola Rieke, Jonny Hancox, Wenqi Li, Fausto Milletari, Holger R Roth, Shadi Albarqouni, Spyridon Bakas, Mathieu N Galtier, Bennett A Landman, Klaus Maier-Hein, et al. 2020. The future of digital health with federated learning. *NPJ digital medicine* 3, 1 (2020), 1–7.

[31] Sebastian Ruder. 2016. An overview of gradient descent optimization algorithms. *arXiv preprint arXiv:1609.04747* (2016).

[32] Micah J Sheller, Brandon Edwards, G Anthony Reina, Jason Martin, Sarthak Pati, Aikaterini Kotrotsou, Mikhail Milchenko, Weilin Xu, Daniel Marcus, Rivka R Colen, et al. 2020. Federated learning in medicine: facilitating multi-institutional collaborations without sharing patient data. *Scientific reports* 10, 1 (2020), 1–12.

[33] Ziteng Sun, Peter Kairouz, Ananda Theertha Suresh, and H Brendan McMahan. 2019. Can you really backdoor federated learning? *arXiv preprint arXiv:1911.07963* (2019).

[34] Hongyi Wang, Kartik Sreenivasan, Shashank Rajput, Harit Vishwakarma, Saurabh Agarwal, Jy yong Sohn, Kangwook Lee, and Dimitris S. Papailiopoulos. 2020. Attack of the Tails: Yes, You Really Can Backdoor Federated Learning. In *NIPS*.

[35] Fangzhao Wu, Ying Qiao, Jiun-Hung Chen, Chuhan Wu, Tao Qi, Jianxun Lian, Danyang Liu, Xing Xie, Jianfeng Gao, Winnie Wu, and Ming Zhou. 2020. MIND: A Large-scale Dataset for News Recommendation. In *ACL*. 3597–3606.

[36] Chulin Xie, Minghao Chen, Pin-Yu Chen, and Bo Li. 2021. Crfl: Certifiably robust federated learning against backdoor attacks. In *ICML*. 11372–11382.

[37] Chulin Xie, Keli Huang, Pin-Yu Chen, and Bo Li. 2020. DBA: Distributed Backdoor Attacks against Federated Learning. In *ICLR*.

[38] Jie Xu, Benjamin S Glicksberg, Chang Su, Peter Walker, Jiang Bian, and Fei Wang. 2021. Federated learning for healthcare informatics. *Journal of Healthcare Informatics Research* 5 (2021), 1–19.

[39] Timothy Yang, Galen Andrew, Hubert Eichner, Haicheng Sun, Wei Li, Nicholas Kong, Daniel Ramage, and Françoise Beaufays. 2018. Applied federated learning: Improving google keyboard query suggestions. *arXiv preprint arXiv:1812.02903* (2018).

[40] Dong Yin, Yudong Chen, Ramchandran Kannan, and Peter Bartlett. 2018. Byzantine-robust distributed learning: Towards optimal statistical rates. In *ICML*. 5650–5659.

[41] Manzil Zaheer, Sashank Reddi, Devendra Sachan, Satyen Kale, and Sanjiv Kumar. 2018. Adaptive methods for nonconvex optimization. *NIPS* 31 (2018).

[42] Xiao Zhang, Zhiyuan Fang, Yandong Wen, Zhifeng Li, and Yu Qiao. 2017. Range Loss for Deep Face Recognition With Long-Tailed Training Data. In *ICCV*. 5419–5428.

[43] Yaoyao Zhong, Weihong Deng, Mei Wang, Jiani Hu, Jianteng Peng, Xunqiang Tao, and Yaohai Huang. 2019. Unequal-Training for Deep Face Recognition With Long-Tailed Noisy Data. In *CVPR*. 7804–7813.

A THERORICAL PROOF

A.1 Proof of Proposition 1

Proof. We analyze benign i_* and malicious i_* separately.

$$\begin{aligned}\mathbb{E}[\sqrt{q}||\mathbf{g}-\boldsymbol{\mu}||_1] \leq & \sum_{\text{benign } i}\mathbb{E}[\sqrt{q^i}||\mathbf{g}^i-\boldsymbol{\mu}||_1\mathbb{I}(i_*=i)] \\ & + \sum_{\text{malicious } k}\mathbb{E}[\sqrt{q^k}||\mathbf{g}^k-\boldsymbol{\mu}||_1\mathbb{I}(i_*=k)],\end{aligned} \tag{1}$$

where q and $\mathbf{g}$ are the quantity and update of selected client i_*.

Lemma 3. *Let $\mathbf{g}^1, ..., \mathbf{g}^n$ be independent identically distributed random vectors with the same quantity q, where $\mathbf{g}^i \subseteq \mathbb{R}^d$, and $\mathbb{E}[\mathbf{g}^i] = \boldsymbol{\mu}$. Supposing that Assumption 1 holds, then we have*

$$\mathbb{E}[\max_i ||\mathbf{g}^i-\boldsymbol{\mu}||_1] \leq \sqrt{2\ln 2n}||\boldsymbol{\sigma}||_1/\sqrt{q}, \tag{2}$$

where $\boldsymbol{\sigma}$ is a d-dimensional vector denoted as $[\sigma_1, ..., \sigma_d]$.

Lemma 3 is proved in Appendix A.5. When i_* is benign, according to Lemma 2 and Lemma 3, we have

$$\begin{aligned}\sum_{\text{benign } i}\mathbb{E}[\sqrt{q^i}||\mathbf{g}^i-\boldsymbol{\mu}||_1\mathbb{I}(i_*=i)] &\leq \mathbb{E}[\max_{\text{benign } i}\sqrt{q^i}||\mathbf{g}^i-\boldsymbol{\mu}||_1] \\ &\leq \sqrt{2\ln 2(n-m)}||\boldsymbol{\sigma}||_1.\end{aligned} \tag{3}$$

When i_* is malicious, the error can be formulated as

$$\begin{aligned}&\sum_{\text{malicious } k}\mathbb{E}[\sqrt{q^k}||\mathbf{g}^k-\boldsymbol{\mu}||_1\mathbb{I}(i_*=k)] \\ &\leq \underbrace{\sum_{\text{malicious } k}\mathbb{E}[\sqrt{q^k}||\mathbf{g}^k-\frac{1}{\sum_{\substack{j:i_*\to j\\ \text{benign } j}}q^j}\sum_{\substack{j:i_*\to j\\ \text{benign } j}}q^j\mathbf{g}^j||_1\mathbb{I}(i_*=k)]}_{\text{Term 1}} \\ &+ \underbrace{\sum_{\text{malicious } k}\mathbb{E}[\sqrt{q^k}||(\frac{1}{\sum_{\substack{j:i_*\to j\\ \text{benign } j}}q^j}\sum_{\substack{j:i_*\to j\\ \text{benign } j}}q^j\mathbf{g}^j)-\boldsymbol{\mu}||_1\mathbb{I}(i_*=k)]}_{\text{Term 2}}.\end{aligned} \tag{4}$$

For Term 1, we have

$$\begin{aligned}&\sum_{\text{malicious } k}\mathbb{E}[\sqrt{q^k}||\mathbf{g}^k-\frac{1}{\sum_{\substack{j:i_*\to j\\ \text{benign } j}}q^j}\sum_{\substack{j:i_*\to j\\ \text{benign } j}}q^j\mathbf{g}^j||_1\mathbb{I}(i_*=k)] \\ &\leq \sum_{\text{malicious } k}\mathbb{E}[\frac{\sqrt{q^k}}{\sum_{\substack{j:i_*\to j\\ \text{benign } j}}q^j}\sum_{\substack{j:i_*\to j\\ \text{benign } j}}q^j||\mathbf{g}^k-\mathbf{g}^j||_1\mathbb{I}(i_*=k)]\end{aligned} \tag{5}$$

Denote $\mathcal{B}$ as the (n-m-2) benign clients with smallest quantities. Since $\sqrt{\frac{q^k}{q^j(q^j+q^k)}} > \frac{1}{q^j+1}$, we have

$$\begin{aligned}&\sum_{\text{malicious } k}\mathbb{E}[\sqrt{q^k}||\mathbf{g}^k-\frac{1}{\sum_{\substack{j:i_*\to j\\ \text{benign } j}}q^j}\sum_{\substack{j:i_*\to j\\ \text{benign } j}}q^j\mathbf{g}^j||_1\mathbb{I}(i_*=k)] \\ &\leq \frac{\max_{\text{benign } i}[q^i+1]}{\sum_{i\in\mathcal{B}}q^i}\sum_{\text{malicious } k} \\ &\mathbb{E}[\sqrt{q^k}\sum_{\substack{j:i_*\to j\\ \text{benign } j}}\sqrt{\frac{q^kq^j}{q^k+q^j}}||\mathbf{g}^k-\mathbf{g}^j||_1\mathbb{I}(i_*=k)].\end{aligned} \tag{6}$$

If $i_*=k$ is selected, it implies for any correct index i

$$\begin{aligned}&\sum_{\text{malicious } k}\sqrt{q^k}[\sum_{\substack{j:i_*\to j\\ \text{benign } j}}\sqrt{\frac{q^kq^j}{q^k+q^j}}||\mathbf{g}^k-\mathbf{g}^j||_1 \\ &+\sum_{\substack{j:i_*\to j\\ \text{malicious } j}}\sqrt{\frac{q^kq^j}{q^k+q^j}}||\mathbf{g}^k-\mathbf{g}^j||_1]\mathbb{I}(i_*=k) \\ &\leq \sqrt{q^i}\sum_{\substack{j:i\to j\\ \text{benign } j}}\sqrt{\frac{q^iq^j}{q^i+q^j}}||\mathbf{g}^i-\mathbf{g}^j||_1 \\ &+\sqrt{q^i}\sum_{\substack{j:i\to j\\ \text{malicious } j}}\sqrt{\frac{q^iq^j}{q^i+q^j}}||\mathbf{g}^i-\mathbf{g}^j||_1.\end{aligned} \tag{7}$$

We focus on the second term of Equation 7. Since any correct index i has $n-m-2$ neighbors and $m+1$ non-neighbors. There exists at least one benign index $\varsigma(i)$, which has Q value score than any of its neighbors. Therefore, $\forall\ j: i\to$ malicious j, $\sqrt{\frac{q^iq^j}{q^i+q^j}}||\mathbf{g}^i-\mathbf{g}^j||_1 \leq \sqrt{\frac{q^iq^{\varsigma(i)}}{q^i+q^{\varsigma(i)}}}||\mathbf{g}^i-\mathbf{g}^{\varsigma(i)}||_1$. Then we have

$$\begin{aligned}&\sqrt{q^i}\sum_{\substack{j:i\to j\\ \text{malicious } j}}\sqrt{\frac{q^iq^j}{q^i+q^j}}||\mathbf{g}^i-\mathbf{g}^j||_1 \\ &\leq m\sqrt{q^i}\sqrt{\frac{q^iq^{\varsigma(i)}}{q^i+q^{\varsigma(i)}}}||\mathbf{g}^i-\mathbf{g}^{\varsigma(i)}||_1.\end{aligned} \tag{8}$$

With Lemma 1, bringing Equation 8 and 7 back to Equation 6, we can obtain

$$\sum_{\text{malicious } k}\mathbb{E}[\sqrt{q^k}||\mathbf{g}^k-\overline{\mathbf{g}}||_1\mathbb{I}(i_*=k)] \leqslant A_{n,m}B_q||\boldsymbol{\sigma}||_1, \tag{9}$$

where

$$\begin{aligned} A_{n,m} &= \sqrt{2\ln 2}(n-m) + m\sqrt{2\ln 2(n-m)}, \\ B_q &= \frac{\max_{\text{benign } i}[q^i+1]\min_{\text{benign } i} i}{\sum_{i\in\mathcal{B}} q^i}, \\ \overline{\mathbf{g}} &= \frac{1}{\sum\limits_{\substack{j:i_*\to j \\ \text{benign } j}} q^j} \sum_{\substack{j:i_*\to j \\ \text{benign } j}} q^j \mathbf{g}^j. \end{aligned} \tag{10}$$

It is easy to prove the following conclusion with the same logic.

$$\mathbb{E}[\sqrt{q}||\mathbf{g}-\overline{\mathbf{g}}||_1 \leqslant A_{n,m}B_q||\boldsymbol{\sigma}||_1. \tag{11}$$

For Term 2, according to Lemma 2 we have

$$\begin{aligned} &\sum_{\text{malicious } k} \mathbb{E}[\sqrt{q^k}||\overline{\mathbf{g}}-\boldsymbol{\mu}||_1 \mathbb{I}(i_*=k)] \\ &\leq \sqrt{\frac{2\ln 2}{\sum_{\substack{j:i_*\to j \\ \text{benign } j}} q^j}} \max_{\text{malicious } i}[\sqrt{q^i}]||\boldsymbol{\sigma}||_1 \\ &\leq \sqrt{\frac{2\ln 2}{\sum_{i\in\mathcal{B}} q^i}} \max_{\text{malicious } i}[\sqrt{q^i}]||\boldsymbol{\sigma}||_1. \end{aligned} \tag{12}$$

Therefore, if all malicious quantities q^i satisfy $q^i \leq \sum_{i\in\mathcal{B}} q^i$, then we have

$$\sum_{\text{malicious } k} \mathbb{E}[\sqrt{q^k}||\overline{\mathbf{g}}-\boldsymbol{\mu}||_1 \mathbb{I}(i_*=k)] \leq \sqrt{2\ln 2}||\boldsymbol{\sigma}||_1. \tag{13}$$

Bring everything back to Equation 1, we have

$$\mathbb{E}[\sqrt{q}||\mathbf{g}-\boldsymbol{\mu}||_1] \leqslant (A_{n,m}B_q + C_{n,m})||\boldsymbol{\sigma}||_1, \tag{14}$$

where $C_{n,m} = \sqrt{2\ln 2(n-m)} + \sqrt{2\ln 2}$.

A.2 Proof of Theorem 2

Proof. Using the smoothness of $F(\cdot)$, we have

$$\begin{aligned} F(\mathbf{w}_{t+1}) &\leq F(\mathbf{w}_t) + \langle \nabla F(\mathbf{w}_t), \mathbf{w}_{t+1}-\mathbf{w}_t\rangle + \frac{L_F}{2}||\mathbf{w}_{t+1}-\mathbf{w}_t||_2^2 \\ &= F(\mathbf{w}_t) + \frac{\eta^2 L_F}{2q_t}||\sqrt{q_t}(\mathbf{g}_t - \nabla F(\mathbf{w}_t)) + \sqrt{q_t}\nabla F(\mathbf{w}_t)||_2^2 \\ &- \frac{\eta}{q_t}\langle \sqrt{q_t}\nabla F(\mathbf{w}_t), \sqrt{q_t}(\mathbf{g}_t - \nabla F(\mathbf{w}_t)) + \sqrt{q_t}\nabla F(\mathbf{w}_t)\rangle \\ &= F(\mathbf{w}_t) + (\frac{\eta^2 L_F}{2} - \eta)||\nabla F(\mathbf{w}_t)||_2^2 \\ &+ \frac{\eta^2 L_F}{2q_t}||\sqrt{q_t}(\mathbf{g}_t - \nabla F(\mathbf{w}_t))||_2^2 \\ &+ (\frac{\eta^2 L_F - \eta}{q_t})\langle \sqrt{q_t}\nabla F(\mathbf{w}_t), \sqrt{q_t}(\mathbf{g}_t - \nabla F(\mathbf{w}_t))\rangle. \end{aligned} \tag{15}$$

Let $\eta = \frac{1}{L_F}$. According to Proposition 1, we further obtain

$$\begin{aligned} &\mathbb{E}[F(\mathbf{w}_{t+1}) - F(\mathbf{w}^*)] \leq \mathbb{E}[F(\mathbf{w}_t) - F(\mathbf{w}^*)] \\ &- \frac{1}{2L_F}\mathbb{E}[||\nabla F(\mathbf{w}_t)||_2^2] + \frac{1}{2q_t L_F}((A_{n,m}B_q + C_{n,m})||\boldsymbol{\sigma}||_1)^2. \end{aligned} \tag{16}$$

Sum up Equation 16, we have

$$\begin{aligned} 0 &\leq \mathbb{E}[F(\mathbf{w}_T) - F(\mathbf{w}^*)] \\ &\leq \mathbb{E}[F(\mathbf{w}^0) - F(\mathbf{w}^*)] - \frac{1}{2L_F}\sum_{t=0}^{T-1}\mathbb{E}[||\nabla F(\mathbf{w}_t)||_2^2] \\ &+ \frac{1}{2L_F}\sum_{t=0}^{T-1}\frac{1}{q_t}((A_{n,m}B_q + C_{n,m})||\boldsymbol{\sigma}||_1)^2, \end{aligned} \tag{17}$$

which implies

$$\begin{aligned} \min_{t=0,\ldots,T}\mathbb{E}[||\nabla F(\mathbf{w}_t)||_2^2] &\leq \frac{2L_F}{T}\mathbb{E}[F(\mathbf{w}_0) - F(\mathbf{w}^*)] \\ &+ \frac{1}{T}\sum_{t=0}^{T-1}\frac{1}{q_t}((A_{n,m}B_q + C_{n,m})||\boldsymbol{\sigma}||_1)^2. \end{aligned} \tag{18}$$

A.3 Proof of Lemma 1

Proof. We first convert the problem into computing expectations of each dimension.

$$\begin{aligned} \mathbb{E}[||\mathbf{g}^i - \mathbf{g}^j||_1] &= \mathbb{E}[\sum_{k\in\{1,\ldots,d\}}|g_k^i - g_k^j|] \\ &= \sum_{k\in\{1,\ldots,d\}}\mathbb{E}[|g_k^i - g_k^j|]. \end{aligned} \tag{19}$$

Since any $z \in \mathcal{D}_i$ are independent, if $|\lambda| < \frac{q^i}{\alpha_k}$, we then have

$$\mathbb{E}[e^{\lambda(g_k^i - \mu_k)}] = \mathbb{E}[e^{\frac{\lambda}{q^i}\sum_{z\in\mathcal{D}_i}(\partial_k f(\mathbf{w};z) - \mu_k)}] \quad \leq e^{\frac{\lambda^2\sigma_k^2}{2q^i}}, \tag{20}$$

which implies g_k^i is sub-exponential with parameters $(\frac{\sigma_k^2}{q^i}, \frac{\alpha_k}{q^i})$, where $\alpha_k < \frac{\sigma_k}{\sqrt{2\ln 2n}}$.

Let $|\lambda| < \min(\frac{q^i}{\alpha_k}, \frac{q^j}{\alpha_k})$. Since g_k^i and g_k^j are independently distributed, we can obtain

$$\begin{aligned} \mathbb{E}[e^{\lambda(g_k^i - g_k^j)}] &= \mathbb{E}[e^{\lambda((g_k^i-\mu_k)-(g_k^j-\mu_k))}] \\ &= \mathbb{E}[e^{\lambda(g_k^i-\mu_k)}]\mathbb{E}[e^{-\lambda(g_k^j-\mu_k)}] \\ &\leq e^{\frac{\lambda^2\sigma_k^2}{2}\frac{q^i+q^j}{q^i q^j}}. \end{aligned} \tag{21}$$

Following the same logic in Lemma 3 and setting $\lambda = \frac{\sqrt{2\ln 2n}}{\sigma_k}\sqrt{\frac{q^i q^j}{q^i+q^j}}$, we can have

$$\mathbb{E}[||\mathbf{g}^i - \mathbf{g}^j||_1] \leq \sqrt{2\ln 2}||\boldsymbol{\sigma}||_1\sqrt{\frac{q^i+q^j}{q^i q^j}}. \tag{22}$$

A.4 Proof of Lemma 2

Proof. As defined in Section 3, we have $g_k^i = \frac{1}{q^i}\sum_{z\in\mathcal{D}_i}\partial_k f(\mathbf{w};z)$. Therefore, we can obtain

$$\mathbb{E}[g_k^i] = \frac{1}{q^i}\sum_{z\in\mathcal{D}_i}\mathbb{E}[\partial_k f(\mathbf{w};z)] = \mu_k, \tag{23}$$

$$\mathbb{E}[(g_k^i - \mu_k))^2] = \mathbb{E}[(\frac{1}{q^i}\sum_{z\in\mathcal{D}_i}\partial_k f(\mathbf{w};z) - \mu_k)^2] = \frac{1}{(q^i)^2}\sum_{z\in\mathcal{D}_i}\mathbb{E}[(\partial_k f(\mathbf{w};z) - \mu_k)^2] = \frac{\sigma_k^2}{q^i}. \tag{24}$$

Since $\partial_k f(\mathbf{w};z)$ is sub-exponential with parameters (v_k^2, α_k), we have

$$e^{\frac{\lambda}{q^i}\sum_{z\in\mathcal{D}_i}(\partial_k f(\mathbf{w};z)-\mu_k)} \le e^{\frac{1}{2q^i}v^2\lambda^2}, \tag{25}$$

when $\lambda \le \frac{q^i}{\alpha_k}$. It shows g_k^i is sub-exponential with parameters $(\frac{v_k^2}{q^i}, \frac{\alpha_k}{q^i})$, where $v_k = \sigma_k$ and $\alpha_k \le \frac{\sigma_k}{\sqrt{2\ln 2n}}$. n is the number of clients sampled by server in each round.

Following the same logic in Lemma 3, we have

$$\mathbb{E}[|g_k^i - \mu_k|] \le \sqrt{2\ln 2}\frac{\sigma_k}{\sqrt{q^i}}. \tag{26}$$

Obviously, we can obtain

$$\mathbb{E}[\mathbf{g}^i] = \boldsymbol{\mu},\ \mathbb{E}[\sqrt{q^i}||\mathbf{g}^i - \boldsymbol{\mu}||_1] \le \sqrt{2\ln 2}||\boldsymbol{\sigma}||_1. \tag{27}$$

A.5 Proof of Lemma 3

Proof. We first convert the problem of computing the expectation of the maximum of the L^1 norm of the d-dimensional vectors into the problem of computing expectations of the maximum of each dimension of the d-dimensional vectors.

$$\mathbb{E}[\max_i ||\mathbf{g}^i - \boldsymbol{\mu}||_1] = \mathbb{E}[\max_i \sum_{k\in\{1,\dots,d\}} |g_k^i - \mu_k|] \le \sum_{k\in\{1,\dots,d\}} \mathbb{E}[\max_i |g_k^i - \mu_k|]. \tag{28}$$

Following the same logic in Appendix A.4, it is easy to prove g_k^i is sub-exponential with parameters $(\frac{v_k^2}{q}, \frac{\alpha_k}{q})$, where $v_k = \sigma_k$ and $\alpha_k \le \frac{\sigma_k}{\sqrt{2\ln 2n}}$. Define $x_k^i = g_k^i - \mu_k$. Denote a list of values $X = \{x_k^1, -x_k^1, \dots, x_k^n, -x_k^n\}$, and $z_k = \max_i |g_k^i - \mu_k| = \max_{x\in X} x$. We then obtain

$$e^{\lambda\mathbb{E}[z_k]} \le \mathbb{E}[e^{\lambda z_k}] = \mathbb{E}[\max_{x\in X} e^{\lambda x}] \le \sum_{x\in X}\mathbb{E}[e^{\lambda x}] \le 2ne^{\frac{\lambda^2\sigma_k^2}{2q}}. \tag{29}$$

$$\mathbb{E}[z_k] \le \frac{\ln 2n}{\lambda} + \frac{\lambda\sigma_k^2}{2q}. \tag{30}$$

Setting $\lambda = \frac{\sqrt{2q\ln 2n}}{\sigma_k} < \frac{q}{\alpha_k}$, we can get

$$\mathbb{E}[z_k] \le \sigma_k\sqrt{2\ln 2n}/\sqrt{q}. \tag{31}$$

Putting Equation 31 back to Equation 28, we obtain

$$\mathbb{E}[\max_i ||\mathbf{g}^i - \boldsymbol{\mu}||_1] \le \sqrt{2\ln 2n}||\boldsymbol{\sigma}||_1/\sqrt{q}, \tag{32}$$

where $\boldsymbol{\sigma}$ is a d-dimensional vector denoted as $[\sigma_1, \dots, \sigma_d]$.

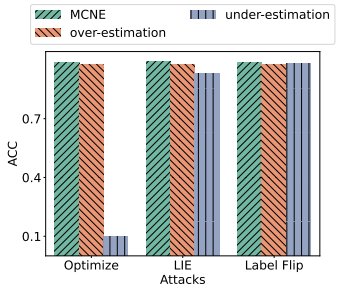

Figure 5: Results of applying malicious client number estimator, under-estimating and over-estimating the number of malicious clients in the IID dynamic-ratio setting on MNIST.

B ADDITIONAL EXPERIMENT

B.1 Distributions of Client Scores

In this subsection, we show some distributions of client scores in our experiments. The distributions support the assumptions in our malicious client number estimator that the scores of benign and malicious clients follow two independent Gaussian distributions, and malicious clients get the largest scores. In Figure 6, we show the distributions of client scores with quantity-enlarge factor $\alpha_q = 10$ at 1,000 steps for MIND, MNIST and CIFAR10 dataset respectively.

C ABLATION STUDY ON MNIST

In this subsection, we compare applying the malicious client number estimator (MCNE) to under-estimating and over-estimating the number of malicious clients $\widetilde{m}$ in the IID dynamic-ratio settings on MNIST. The results are shown in Figure 5 The performance of experiments with MCNE is consistently higher than those with over-estimation and under-estimation. This is because the number of malicious clients follows a hypergeometric distribution in the dynamic-ratio setting, which is hard to be estimated by a fixed parameter. Under-estimating the number of malicious clients makes some malicious clients selected in some rounds, while over-estimation filters some benign clients in most rounds.

D EXPERIMENTAL ENVIRONMENTS

We conduct experiments on a single V100 GPU with 32GB memory. The version of CUDA is 11.1. We use pytorch 1.9.1.

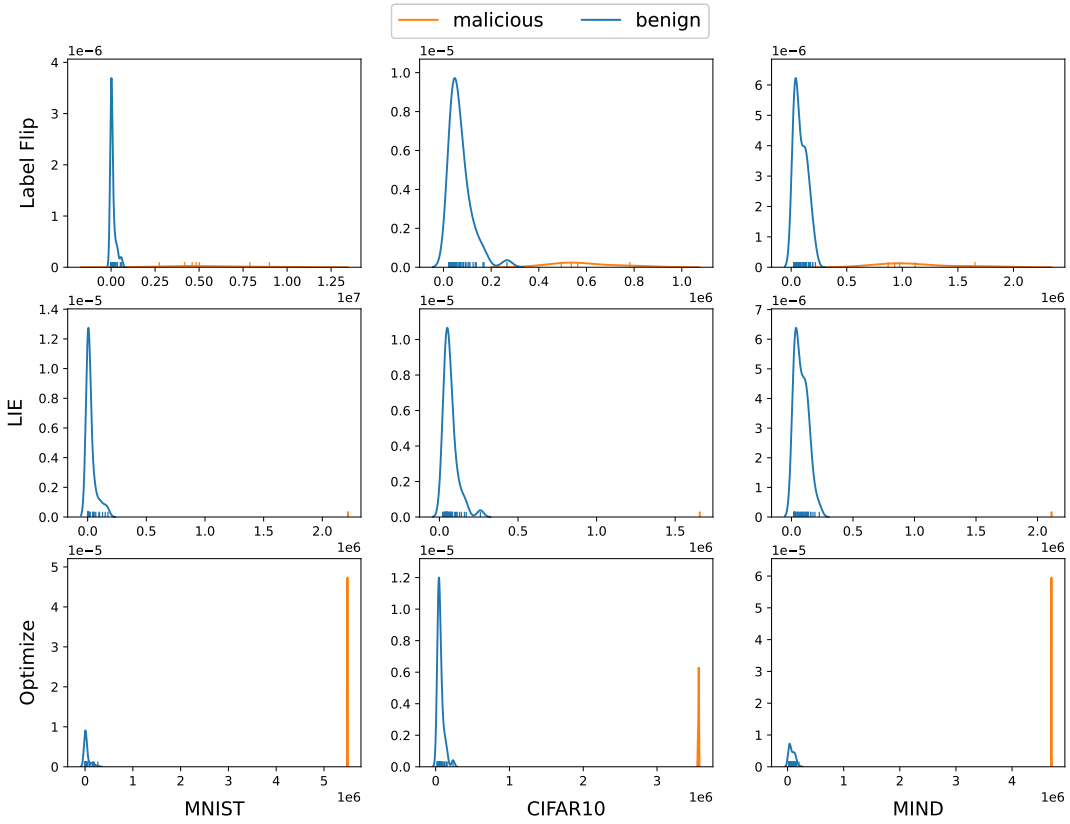

Figure 6: Distributions of client scores in IID dynamic-ratio settings at 1,000 steps.